Metamodel-based Design Optimization of Structural One-way Slabs based on Deep Learning Neural Networks to Reduce Environmental Impact

Javier Ferreiro-Cabello[1], Esteban Fraile-Garcia[1], Eduardo Martinez de Pison Ascacibar[1], Fco. Javier Martinez de Pison Ascacibar[2].

Esteban Fraile-Garcia. Email: esteban.fraile@unirioja.es

Javier Ferreiro-Cabello. Email: javier.ferreiro@unirioja.es

Eduardo Martinez de Pison Ascacibar. Email: eduardo.mtnezdepison@unirioja.es

Fco. Javier Martinez de Pison Ascacibar. Email: fjmartin@unirioja.es

(1) University of La Rioja (Spain), Department of Mechanical Engineering, SCoDIP Group.
(2) University of La Rioja (Spain), Department of Mechanical Engineering, Edmans Group.

Corresponding author: Javier Ferreiro-Cabello, University of La Rioja, Department of Mechanical Engineering. C/San José de Calasanz 31, 26004 Logroño (Spain). Email: javier.ferreiro@unirioja.es.

Abstract

This article presents a methodology for the construction and use of metamodels with Deep Learning (DL) methods that are useful for making multi-criteria decisions in the design and optimization of one-way slabs. The main motivation behind this research has been to examine the possibilities of improving slab design by including this methodology in future tools, which is capable of calculating thousands of solutions in real time based on the designer's specifications. The process of creating these metamodels begins by developing a database of millions of combinations of slab designs. These combinations are calculated with a heuristic algorithm that provides the following results: rigidity, deflection, cost per square meter, CO_2 emissions and embodied energy. Once a database including the entire universe of possible solutions has been created, a metamodel is developed that is capable of "condensing" the implicit knowledge contained in the database. This metamodel is included within a Decision Support System (DSS) that produces thousands of solutions for slabs that all comply with a range of specifications designated by the design plan. Furthermore, the methodology described herein proposes the use of Pareto-optimal solutions and graphic tools to help designers make multi-criteria decisions regarding the solutions that best fit their needs. A case study is presented to illustrate this proposal: optimizing slab design in two buildings according to technical, economic and sustainability criteria. The results indicate that the multi-criteria solutions obtained would entail a significant reduction in both emissions and embodied energy as compared to mono-criteria solutions, without significantly increasing costs.

Keywords

One-way slab, Deep Learning, Multicriteria optimization, Metamodel, Structures, Reinforced concrete.

1. INTRODUCTION

The construction industry constitutes a business sector that consumes great quantities of energy while also emitting large amounts of CO_2. Breaking down this consumption, building a reinforced concrete structure represents between 59.57% and 66.73% of the total energy consumed [1]. Likewise, a building's use phase represents a large part of total CO_2 emissions. Therefore, much research in recent years has focused on improving the energy efficiency of building operation [2]. And as the Net Zero Energy Building concept spreads rapidly, reducing CO_2 emissions and the amount of energy consumed during the manufacture of construction materials is also gaining importance. Thus, adequate design of reinforced steel elements must consider energy consumption and emissions generated during material production.

Over the past few decades, numerous studies have investigated optimizing the design of reinforced steel elements in terms of cost and emissions. For example, Park et al. [3] applies genetic algorithms (GA) to design composite columns in high-rise buildings (35 stories) and identifies specific dimensions and reinforcements that reduce cost and CO_2 emissions. Another study focuses on designing bridge piers and uses hybrid multi-objective simulated annealing (SA) algorithms, and incorporates the aforementioned objective functions (cost and emissions), as well as reinforcing steel congestion [4]. Two studies on designing reinforced concrete footings that reduce cost and CO_2 emissions should be mentioned. The first study utilizes the optimization methodology known as Big Bang-Big Crunch to optimize isolated footings in accordance with the specifications prescribed by the American Concrete Institute (ACI 318-11) [5]. The second study develops a new method called hybrid firefly algorithm (FA) to apply to spread footing [6]. Regarding the optimum design of reinforced concrete retaining walls, Khajehzadeh et al. [7] present and apply a new version of the gravitational search algorithm based on opposition-based learning (OBGSA). In this same line of research, Yepes et al. [8] present an approach to a methodology using a hybrid multistart optimization strategic method based on a variable neighborhood search threshold acceptance strategy (VNS-MTAR) algorithm. Another study examines a different reinforced concrete component subject to bending stress: high performance concrete for simply supported beams is designed using the same VNS algorithm [9]. And lastly, Paya-Zaforteza et al. implement a SA algorithm [10] to examine combinations of compression and stress components (columns and beams) according to Spanish building code. All these studies demonstrate the complexity involved in creating building designs that cut down on costs and emissions.

In the case of concrete slabs, how to reduce costs through better design has been studied extensively. An example of such a study can be found in the research of Merta and Kravanja [11] who include labor costs in overall manufacturing costs. Another study conducted by Tabatabai and Mosalam [12] demonstrates how two programs, designed for two separate tasks, can be integrated in an environment for performance-based reinforcement design that guarantees cost-effectiveness through optimization and structural safety through satisfying serviceability conditions. Kaveh et al. also conduct various studies focused on optimizing costs in

the design of one-way reinforced concrete slabs. For example, their first study uses a harmony search algorithm and also conducts a parametric study examining the effects of beam span and loading [13]. In a later study, the authors include the materials used and the construction cost of the structure in the objective function. In this case, optimization is carried out by the improved harmony search (IHS) algorithm and the results are compared to those of the charged system search (CSS) [14]. These same authors, in another later study, compare and evaluate the capacities of several metaheuristic algorithms for optimizing the costs of a concrete slab [15]. **En 2016 Kaveh y Ghafari, han analizado una estructura hibrida de acero y hormigón, en este caso la optimización de la función coste total is performed by enhanced colliding body optimization (ECBO)** [16]**.** Similarly, Ahmadi-Nedushan and Varaee [17] evaluate the performance of different algorithms and demonstrate that particle swarm optimization (PSO) is a promising method for design optimization of structural elements. Other studies point out the need to incorporate additional parameters into design criteria. For example, Liébana et al. [18] analyze CO_2 emissions generated by different construction techniques, Del Coz et al. [19] incorporate thermal behavior in their proposal, and Fraile-García et al. [20] consider life cycle assessment (LCA) in the design of reinforced concrete structures.

In recent years, various decision support systems (DSS) have been developed that use machine learning models to support structural design and maintenance. For example, some research has investigated how to improve the prediction of shear resistance performance in large span beams using support vector machines (SVM) [21] or artificial neural networks (ANN) [22]. Other studies optimize the design of beams without stirrups through evolutionary polynomial regression [23] or gene expression programming (GEP) [24], with the objective of adapting those formulas included in the regulations. Other variables studied in relation to concrete are as follows: compressive strength through ANN [25][26], compressive strength of high performance concrete with adaptive network-based fuzzy inference system (ANFIS) [27], and tensile strength with GEP [28], creep with ANN [29], and abrasive wear with various models based on ANN, fuzzy logic model with genetic algorithm and general lineal models (GLM) [30]. In all of these studies, the models are tested with experimental testing data and demonstrate satisfactory results. Other authors, on the other hand, utilize models to determine risk factors and corrective measures for infrastructure. For example, Cheng and Hoang [31] estimate the risk score for bridge maintenance with the evolutionary fuzzy least squares SVM. Okasha and Frangopol also [32] develop an advanced model for life-cycle performance prediction and service-life estimation of bridges. Similarly, because reinforced concrete structures are subject to corrosion, tools have been proposed to support decision-makers in planning maintenance interventions with the fuzzy time-dependent method [33] or through ANN whose weights are optimized with an imperialist competitive algorithm (ICA) [34].

As more parameters are incorporated into structural design, the decision-making process becomes more complex. Thus, Yepes et al. [35] optimizes bridge design based on economic, structural security and environmental sustainability objectives. Castilho and Lima [36] utilize genetic algorithms (GA) to minimize

the costs of continuous one-way slabs in which the concrete characteristics and joist spacing are varied. Hailong Zhao et al. [37] incorporate a greater number of design variables and construction factors and employ metamodels applied to the structural design of metal trusses to effectively reduce the computational time necessary. Gharehbaghi and Khatibinia [38] utilize metamodels trained with real data to optimize seismic design. Another study illustrates the effectiveness of using metamodels to design concrete barriers [39].

All the above-mentioned studies are based on machine learning methods, or evolutionary and bio-inspired methods of optimization. Within this field, research conducted in recent years with deep learning (DL) has advanced the design of support systems for the decision-making process. This type of technique, many of which having evolved from ANN, aim to model information with various levels of abstraction by using different non-linear interconnected layers. Among the diverse DL techniques, architectures corresponding to "deep neural networks" (DNN) are those techniques most used in supervised modeling. In this case, DNN are artificial neural networks (ANN) formed by multiple layers of neural networks with a high number of non-linear neurons per layer. Thus, DNN are often comprised of by three, four or more layers, with thousands of neurons in each one. These types of networks are very flexible which allows them to handle complex problems, but their downside is the risk of overfitting through training, and therefore losing their capacity to adequately explain the problem. To avoid this problem, current DNN training algorithms incorporate a range of mechanisms to reduce the risk of overfitting models.

Keeping in mind the current tendency to implement building information modeling (BIM) systems for structures, agile tools are necessary to make decisions during the design phase. Given this situation, combining structural analysis tools with search and optimization algorithms is considered a promising option [40].

This study proposes a methodology to develop metamodels based on deep-learning methods capable of working with multiple combinations of one-way slab design options to predict in real time: rigidity, deflection, cost per square meter, embedded energy and CO_2 emissions. These metamodels combined with other types of methods such as Pareto-optimal solutions or graphic tools can be included in decision support systems (DSS) to design and optimize one-way slabs. Such DSS can be useful for selecting the optimal design of slabs from a multi-objective point of view that takes into consideration technical, economic and sustainability criteria.

2. METHODOLOGY

2.1. Decision Support System based on Deep Learning Techniques

The decision support system (DSS) is based on a metamodel developed with deep learning (DL) techniques to optimize the structural design of one-way slabs in terms of economic, technique and sustainability criteria. The DSS incorporates a DL-metamodel (MetaDL) that is capable of quickly extracting thousands of construction solutions from stipulations indicated by the designer. Likewise, the DSS has search algorithms based on Pareto-optimals that limit the number of final solutions so that the designer is able to analyze them. To facilitate analysis of these solutions, the DSS includes graphic tools such as dendrograms and scatterplots that assist designers in choosing the most adequate solution for their proposals.

2.2 Construction of the MetaDL

The process of creating the MetaDL is illustrated in Figure 1. First, a heuristic algorithm based on current construction methodology and international regulations creates a database of thousands of construction solutions. This database includes millions of hypothetical designs covering the entire range of possible solutions. Then, five DNN models are trained and validated in order to obtain a precise metamodel capable of assimilating and synthesizing the implicit knowledge contained in the universe of solutions presented. Thus, the final objective is to achieve a sufficiently precise metamodel that can substitute the heuristic algorithm and be utilized during the decision-making phase. The primary advantage of MetaDL, in comparison to the heuristic algorithm, is that it allows designers to compare, in real time, thousands of different construction solutions for a specific design case. Among these solutions, selecting the Pareto-optimal solutions considerably reduces the number of final solutions so that the designer may visually analyze them. Hence, incorporating MetaDL into the DSS allows designers to choose the best solutions, in terms of construction and sustainability, from thousands of possibilities.

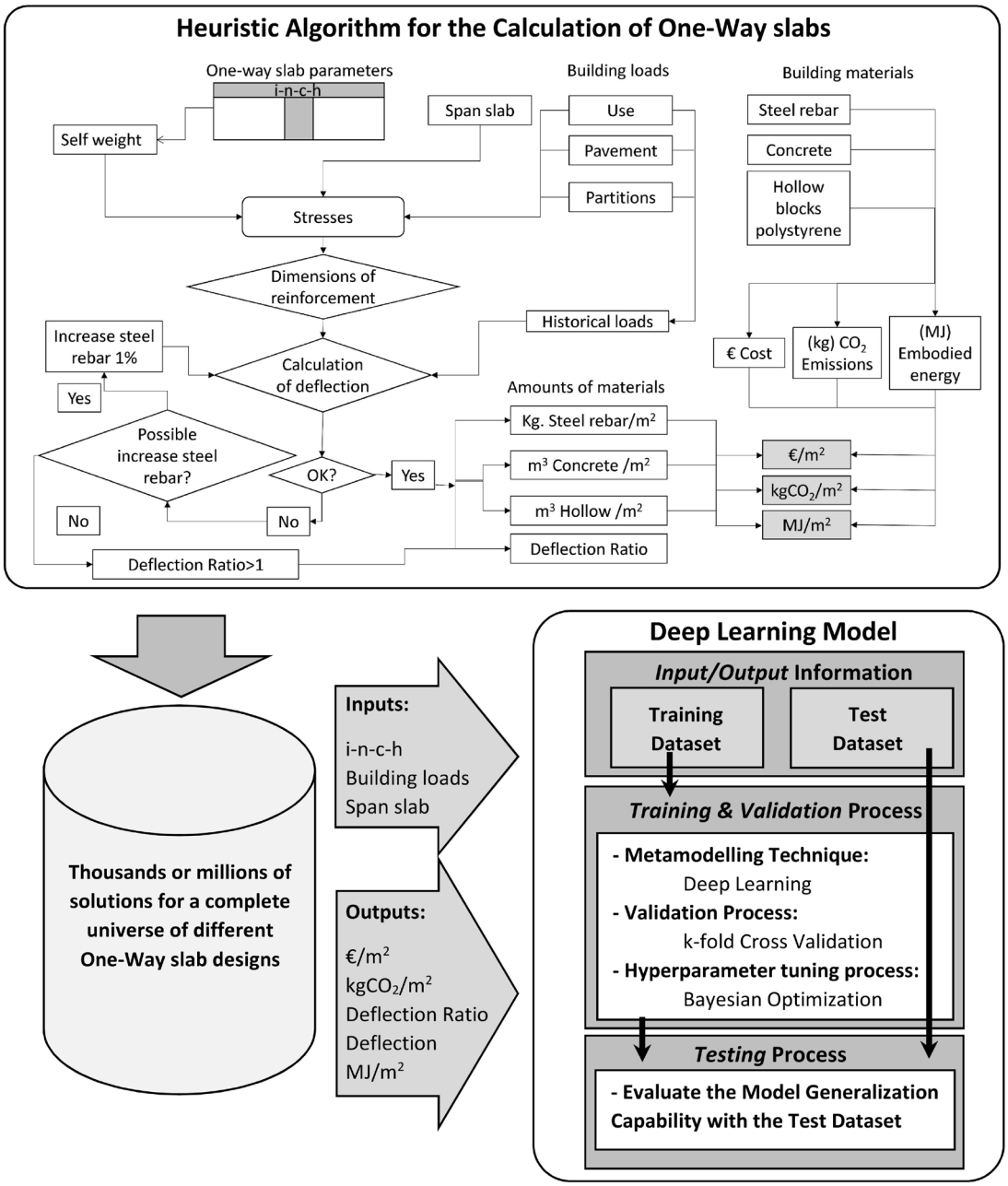

Figure 1 Building stages for MetaDL for a DSS in the design of one-way slabs.

2.3 Heuristic Method for Calculating One-way Slabs

To implement the design proposals for one-way slabs and not place any limits on the possible solutions' geometry, hollow blocks made of expanded polystyrene are utilized. Therefore, the slab's geometry can be modified by adjusting the blocks' dimensions, meaning that the design is flexible since the rib width and compression layer can be modified while maintaining the same total thickness.

The algorithm to calculate and design the one-way slabs is realized for a T-shaped section (Figure 2). The T-shaped design is affected by four parameters: Effective flange width is taken as half the distance between ribs, inter-axis (i), in-situ rib width (n), compression layer (c), and height of the hollow block (h). Therefore, each design solution for a slab section is referred to by the following term: **i-n-c-h**. In addition to these four

variables that define the slab section, four input variables corresponding to spans and typical building loads are incorporated: use, pavement, and partitioning. To sum up, eight input parameters are considered for each design: inter-axis (i), rib (n), compression layer (c), height of hollow block (h), span, live load, pavement load, and partition load.

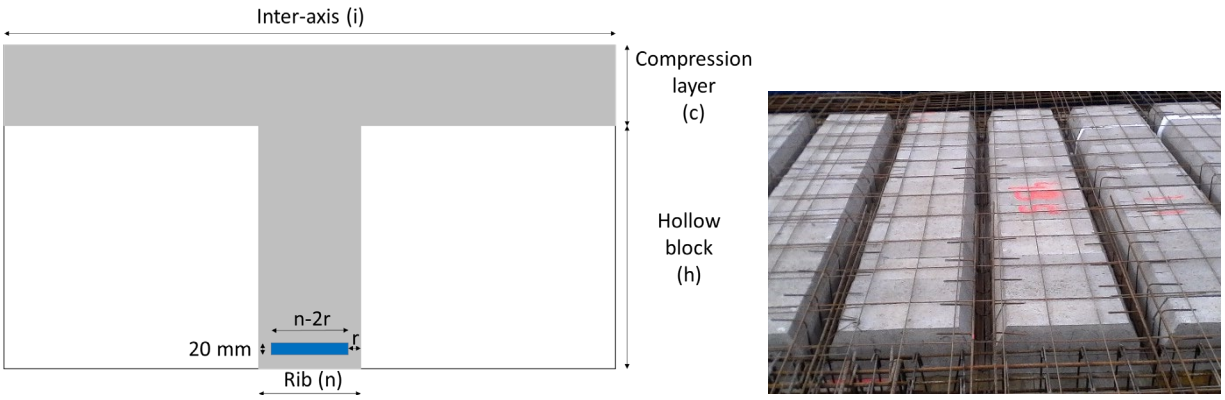

Figure 2. Design parameters for one-way slabs.

The calculations are performed for each solution, and the output variables obtained are cost, deflection, the ratio of deflection compared to the maximum acceptable deflection, CO_2 emissions, and embodied energy per square meter of each solution (**i-n-c-h**).

The upper section of Figure 1 describes the heuristic algorithm used to calculate each construction solution. This algorithm has two distinct parts: the structural analysis of the solution and the evaluation of economic and environmental costs.

Now, let us outline the structural analysis process. First, the variables "i-n-c-h" are defined, which correspond to the geometry of the T-section, and then by referencing the density of the materials (reinforced concrete 2.5 kN/m^3 and expanded polystyrene 0.15 kN/m^3), the weight of the slab can be calculated. Then, once the loads (use, pavement, partition) and span are determined, the stresses for each specific case are obtained. In this case, current regulations require that for simple supports (null moment) a negative moment of 25% of the span which it supports is considered. By implementing the formula included in the regulations [41] , **que incorpora las directrices de la norma europea EN 1992-1-1 para proyectos de estructuras de hormigón**, regarding the T-sections' dimensioning, the necessary reinforcements are established. Once the exact reinforcements necessary for adequate strength are defined, the deflection can be verified. **Se ha establecido el límite superior para armadura de refuerzo de 20x(n-2r) mm^2 respetando un recubrimiento de 30 mm (figura 2)**. For this study, a history of loads based on common construction practices in Spain was established. To this end, four types of loads were established according to the purpose of the different loads: self weight, partition, floor covering, and live load. In reinforced concrete structures, the values for active and total deflection in structural components must be monitored given that the deflection of these components affects those elements considered non-structural. The deflection which takes place after the application of

finishes or fixing of partitions should not exceed span/400 to avoid damage to fixtures and fittings. This deflection consists of two types of deflections: instantaneous and time-dependent, as indicated in Figure 3.

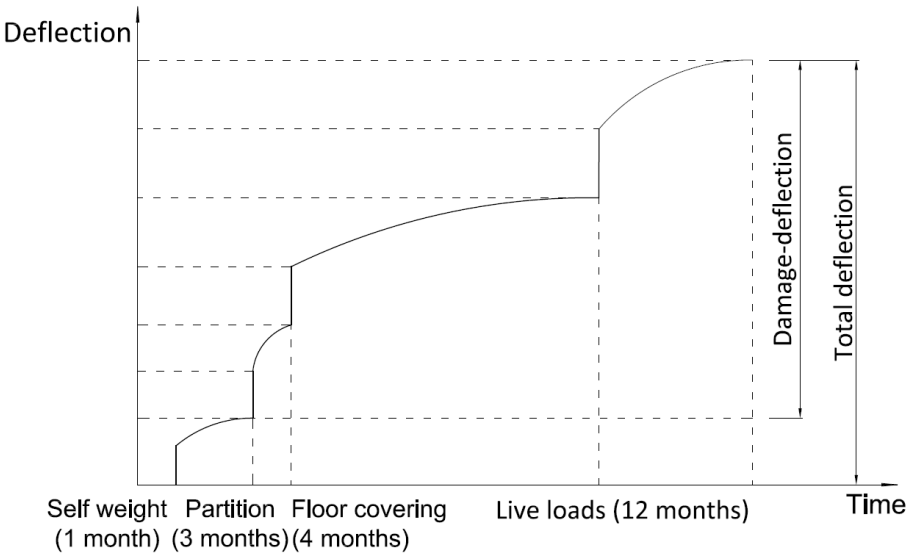

Figure 3. Evolution of deflection for history of loads.

The damage-deflection of a structural element in reference to a damageable non-structural element, is the deflection value obtained in the first element due to the construction of the second. Total long-term deflection is the sum of damage-deflection plus the deflection of the structural element occurring up until the damageable element is constructed.

In this study, the damageable elements are the partitions and the floor coverings, and the structural element is the slab. To calculate the equivalent inertia (I_e) of the slab in question, the Branson formula [41] is implemented:

$$I_e = \left(\frac{M_f}{M_a}\right)^3 \cdot I_b + \left[1 - \left(\frac{M_f}{M_a}\right)^3\right] \cdot I_f \leq I_b \qquad (1)$$

In which:

M_a: Maximum bending moment applied to the section until the instant when the deflection is calculated.

M_f: Nominal cracking moment of the section.

I_b: Moment of inertia of the gross section.

I_f: Moment of inertia of the simply bent cracked section.

This inertia value models the presence of cracking when the materials are subject to loads; and instant deflection is obtained by means of the material strength formulas. To calculate the different deflections, a

simplified calculation that is included in the regulations is utilized, using the factor ξ , a coefficient that depends on the load time and the takes the following values according to the time (Figure 4).

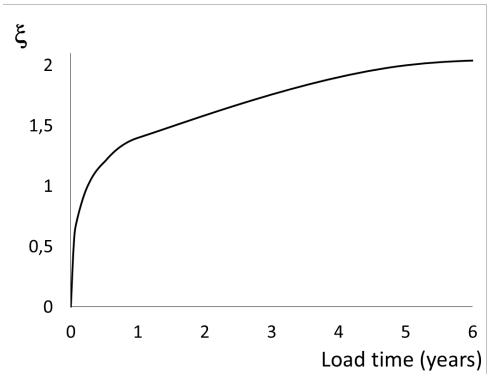

Figure 4. Coefficient ξ to calculate time-dependent deflection.

To calculate the deflection of instant t_f for the age of the load t_c, the value to be considered is:

$$\xi = \xi(t_f) - \xi(t_c) \quad (2)$$

The values of maximum acceptable deflection are implemented as relative values: L/400 for damage-deflection and L/250 for total deflection, L represents the centimeters of span. The definition of the reinforcements obtained for strength is used as a basis the first time the deflection is checked. A cycle comes into play wherein if the section's features must be improved because they do not comply with the deflection limits, a gradual calculation is conducted with 1% increases in the reinforcement sections. **Estos incrementos de la armadura permiten reducir la fisuración y de esta forma incrementar la inercia equivalente, al aplicar la fórmula de Branson, para una misma sección de hormigón**. This cycle to redefine reinforcements has two established limits: deflection cannot fall below the maximum admissible values nor can it reach a quantity of steel that would be impossible to incorporate into the section. Therefore, each iteration of the cycle must check the viability of the reinforcement.

Obtaining the definitive reinforcements for each solution provides us with information regarding the quantities of materials required for each solution. These quantities are all based on a square meter of the solution, but in different quantities depending on the material in question. Thus, the measurement for reinforced steel is kg/m^2; for concrete, m^3/m^2; and for expanded polystyrene, $m^3/^{m2}$. In addition, the ratio of deflection is also recorded (maximum deflection/acceptable deflection). Cases wherein this ratio is greater than the unit are deemed invalid as they surpass the admissible amount of deflection.

The second part of the algorithm implements the economic and environmental costs of the corresponding solution. In order to do so, the following databases are referenced: Ecoinvent [42], Bedec [43], CYPE [44]),

and on a sector level, some Environmental Product Declarations for steel [45], concrete [46] and expanded polystyrene [47]. Table 1 was created based on these databases.

Amount /Material	Cost (€)	Emissions CO_2 (kg)	Embodied Energy (MJ)
Kg / Steel Rebar	1.0	3.16	55.0
m^3 / Concrete (HA-25-B-20-IIa)	93.0	235.8	2424.0
m^3 / Expanded Polystyrene δ=0.15kN/m^3	45.0	44.8	1325.0

Table 1 Economic and environmental cost per unit.

Information provided by the figures for material usage allows us to obtain the economic and environmental costs of each solution studied herein.

2.4. Generating the Results Database

This algorithm is used to generate a database of solutions. From the original problem's eight parameters, the density of the cases studied is increased in the i-n-c-h parameters by varying the loads and span with less intensity. Table 2 includes detailed information. Maximum and minimum values are deliberately increased to improve the training of the model in regards to the limits of possible solutions.

Parameter	Minimum	Maximum	Increases
Inter-axis (i)	50 cm	100 cm	5 cm
Rib cast-in-place (n)	10 cm	26 cm	2 cm
Compression-Layer (c)	4 cm	8 cm	1 cm
High hollow block (h)	10 cm	40 cm	3 cm
Span one-way slab	350 cm	650 cm	50 cm
Live Loads	0 kN/m^2	4 kN/m^2	2 kN/m^2
Load of Pavement	0 kN/m^2	2 kN/m^2	1 kN/m^2
Load of Partitions	0 kN/m^2	2 kN/m^2	1 kN/m^2

Table 2. Input Parameters. Ranges and increments.

Utilizing the heuristic algorithm with a combination of input parameters found in Table 2, the following outputs are obtained: economic cost in €/m^2, energy necessary to obtain the solution in MJ/m^2, CO_2 emissions in kg/m^2, deflection rate (maximum ratio of estimated deflections to maximum admissible deflection) and the estimated damage-deflection in centimeters. Therefore, a grid is generated of all the possible combinations based on the input parameters listed in Table 2 and according to the ranges and intervals assigned to each one. The results correspond to the total possible combinations of: 11 intera-xis, 9 ribs, 5 compression layers, 11 high hollow blocks, 7 spans, 3 live loads, 3 loads of floor covering and 3 loads of partition. That is, 11x9x5x11x7x3x3x3=1029105 construction solutions.

2.5. Training and Validating the Metamodel based on Deep Learning techniques

2.5.1. Deep Learning

Once the database is developed, five DNN are trained, one for each output. To avoid overfitting during the training process and to obtain models that are good at generalizing the problem to be explained, DNN

algorithms nowadays incorporate various regularizing parameters. For example, penalties of type L1 (Lasso) or L2 (Ridge) modify the loss function based on the model's complexity. Other techniques to limit overfitting use “drop-out” parameters to reduce the number of connections in the neural networks in inputs as well as in the hidden layers. These techniques are especially useful when working with high dimensional or noisy databases, because they reduce anomalous or unnecessary dependencies. Furthermore, with other types of parameters one can randomly select a sub-space of characteristics (random-subspaces method) in each iteration, or reduce the number of samples with the aim of minimizing the final variance error (similar to approaches such as bagging). Thus, the training process focuses on adjusting various parameters, some of which serve to minimize the objective function and others, to avoid over-fitting through intrinsic processes similar to sub-sampling, feature selection, regularization, etc.

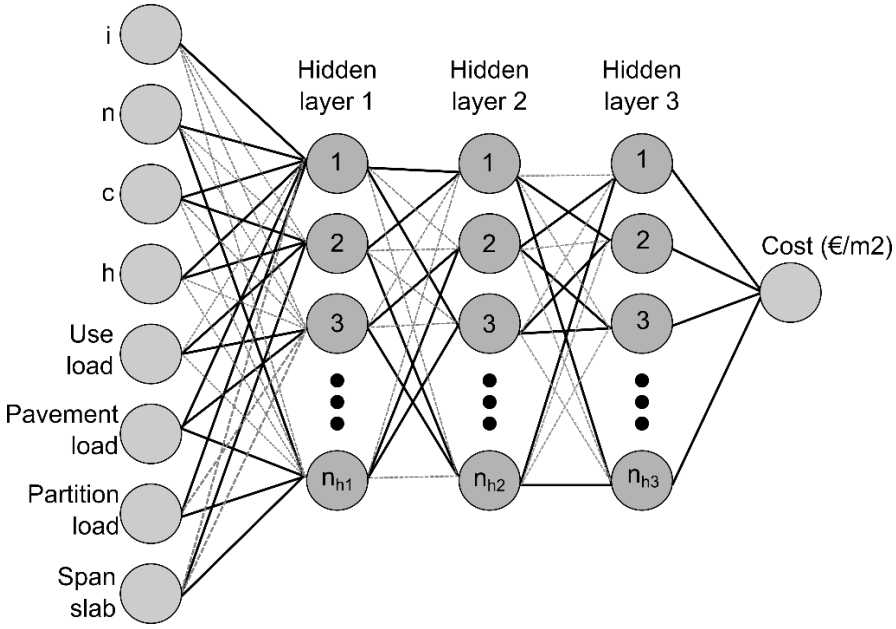

Figure 5 Example of DNN to estimate the cost per square meter of slab wherein a drop-out process is realized in each training iteration to disconnect connections between neurons with the objective of avoiding overfitting the model.

2.5.2. Creation of the Metamodel

The metamodel consists of five DNN models. Each DNN is capable of predicting one of the output variables, based on eight input variables. **La Figura 5 muestra la topología de DNN utilizada para predecir el coste. Para los cinco casos, la estructura de la DNN es similar y está basada en un feed-forward neural network con una capa de entrada, 3 capas ocultas y una de salida que corresponde a la variable dependiente. Para cada modelo, lo único que varía es n_{h1}, n_{h2}, y n_{h3} que definen respectivamente el número de neuronas de las capas ocultas 1, 2 y 3.**

Para la definición de esta topología, inicialmente se realizaron diversas pruebas para prefijar el número de capas, el tipo de función de activación de las neuronas, la ratio de aprendizaje (*learning_rate*) y el porcentaje de conexiones de cada capa que son desactivadas en cada *training stage* (*drop_out*), y que sirve

para prevenir el sobreentrenamiento de la DNN (*overfitting*). Para conseguir unos tiempos de entrenamiento aceptables, los mejores errores preliminares de validación se obtuvieron al fijar el número de capas a 3, el *drop_out* de todas las capas a 0.5, el *learning_rate* a 0.005; y usando funciones de activación del tipo "relu" y parada temprana (*early_stopping*) de 10 epochs. Finalmente, el proceso de ajuste fino de los modelos DNN se basó en la selección del número más adecuado de neuronas de cada una de las capas ocultas y del ajuste del *momentum*, tal y como se explica en el punto 3.2

The process of training the DNN begins by dividing the database into two parts. 70% of the cases are selected at random from the database for training and validation. The other 30% is reserved for the testing stage. The database is utilized exclusively to verify the generalization capacity of each of one the selected models.

To facilitate training the DNN model, a z-score normalization is realized on each of the variables from the database through the following expression:

$$A_i' = \frac{A_i - \bar{A}}{\sigma_A} \tag{3}$$

where $\bar{A}$ is the mean of the variable A and σ_A is the standard deviation.

The validation process is carried out by a k-fold cross validation (CV) which consists of dividing the dataset into k subsets. In each iteration, k-1 subsets are used for training the model and a partial error is obtained with the subset not selected. The procedure is repeated k times selecting a different validation subset in each iteration. The final cross-validation error is calculated with the arithmetic mean of the k partial sample errors. In this study, *k* is equal to 5 and the root mean square error (RMSE) is used as the validation error, where:

$$RMSE = \sqrt{\frac{\sum_{i=1}^{n}(y_i - \tilde{y}_i)^2}{n}} \tag{4}$$

y_i and $\tilde{y}_i$ are respectively, the actual and the predicted output of the i solution and n, the number of samples in each validation subset.

A random search is conducted for the best DNN model wherein the following parameters are modified: the number of neurons in each hidden layer (n_{h1}, n_{h2} y n_{h3}), and then momentum, learning_rate and drop_out of each of the hidden layers. Moreover, early_stopping is used to avoid overtraining.

2.6 Applying the MetaDL to obtain the best design solutions

Once the MetaDL is trained and validated, designers can use it in practical cases to select construction solutions from the range of designs they deem appropriate and by establishing the live loads beforehand.

From among these solutions, the DSS obtains the optimal Pareto solutions: this sub-group of the total solutions represents the best solutions because the other solutions do not improve one objective without adversely affecting another objective. Utilizing the Pareto-optimal solutions considerably reduces the number of solutions to be examined in multi-criteria problems. And finally, the DSS incorporates graphic tools such as dendrograms and scatterplots that help to select the solution that best suits the problem's conditions.

3. CASE STUDY. RESULTS AND DISCUSSION

3.1 Description of Case Study

To compare and contrast the suitability of the model proposed, the aforementioned methodology is applied in a mono-criteria and multi-criteria optimization of two different buildings. The objective is to demonstrate the viability of the methodology in common structural design processes.

Given that the ultimate goal is to determine the optimum design for a slab section (i-n-c-h), the geometric parameters and buildings loads must be established. The geometric parameters depend on the building's architectural design, wherein the span between columns varies. In this study, two buildings are examined that simulate two realistic situations: building Y with a span of 420 cm and building Z with a span of 580 cm. **El caso de estudio, se realiza para forjados aislados de un único vano, aportando resultados para diferentes valores de las solicitaciones**. In both cases, the roof spans increased considering a 30% slope, which results in 440 and 606 cm respectively. The loads considered for each floor, in addition to self-weight, depend on their designated use. The most common uses are: parking garages, commercial use, dwellings, storage rooms and roofs. In the proposed models, these loads are divided into three concepts: use loads vary between 4 and 1 kN/m^2 and are established according to the use of the slab, pavement loads are between 0 and 1 kN/m^2 and correspond to the weight of the roof materials placed on top of the slab, and the partition load ranges between 0 and 2 kN/m^2. Figure 6 shows the geometry and loads considered for each building.

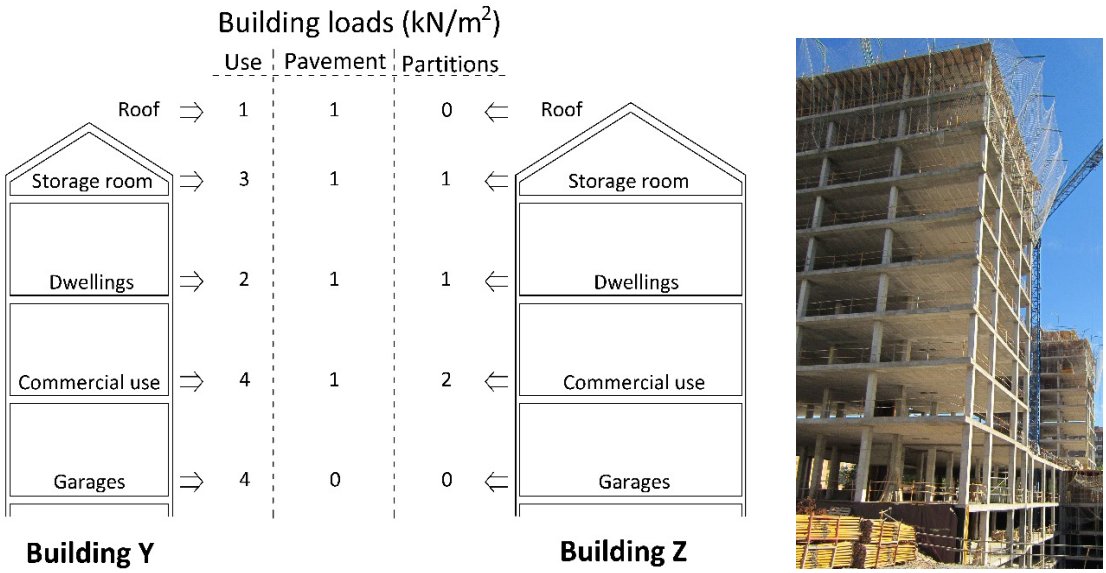

Figure 6. Case study.

Designers usually decide on a single slab design as the structural solution for a building. Thus, a typical slab design was selected for both buildings (Y and Z) with the following i-n-c-h code: 72-12-5-25. Table 3 shows to results obtained for each building and each floor.

	Building Y				Building Z			
	€/m²	MJ/m²	kgCO₂/m²	Ratio of deflection	€/m²	MJ/m²	kgCO₂/m²	Ratio of deflection
R	19.55	588.91	36.16	0.10	20.26	628.18	38.41	0.97
SR	19.95	611.03	37.43	0.38	25.89	937.80	56.20	1.00
D	19.72	598.15	36.69	0.23	24.22	845.86	50.91	1.00
CU	20.40	635.59	38.84	0.76	29.27	1123.75	66.88	1.00
G	19.76	600.73	36.83	0.21	23.53	808.13	48.75	1.00

R: Roof, SR: Storage room, D: Dwellings, CU: Commercial use, G: Garages.

Table 3. Economic and environmental analysis and ratio of deflection for structural solution 72-12-5-25.

3.2 Creating the MetaDL

The MetaDL obtained consists of five DNN models that precisely predict each of the five output variables described above. The topology of each DNN model was established in three hidden layers, setting drop_out at 0.5, and the learning_rate at 0.005. The search process for the best model was conducted by selecting the number of neurons for the first two layers as 256, 512, or 1024; whereas for the third hidden level, the size was reduced to a selection among the following values: 8, 16, 32, 64 or 128. The momentum was established within a range of 0.5 and .095 at random.

All experiments were realized with the statistical software R and the MXNet Deep Learning package. The server was a Z230 HP-Workstation with a Tesla K40 GPU Card.

Table 4 shows the parameters for the best DNN model obtained for each output variable, where n_{h1}, n_{h2} and n_{h3} correspond respectively to the number of neurons in hidden layers 1, 2, and 3. The dropout for the three layers was set at 0.5. The last two columns show the learning_rate and the momentum.

Model DNN	n_{h1}	n_{h2}	n_{h3}	*Dropout1*	*Dropout2*	*Dropout3*	*Learning Rate*	*Momentum*
Cost (€/m²)	256	1024	16	0.5	0.5	0.5	0.005	0.726322
Energy (MJ/m²)	1024	1024	16	0.5	0.5	0.5	0.005	0.698062
CO_2 ($kgCO_2/m^2$)	512	1024	16	0.5	0.5	0.5	0.005	0.567881
Rigidity	512	1024	16	0.5	0.5	0.5	0.005	0.567881
Deflection (cm)	512	512	8	0.5	0.5	0.5	0.005	0.768566

Table 4. Parameters of the best models obtained for each output variable.

100 models were trained for each output and that which had the least 5-fold CV RMSE ($RMSE_{CV}$) was selected. Table 5 shows the results obtained for each of the DNN models. The second and third columns show the range for each of the output variables. The fourth column lists the $RMSE_{CV}$ which corresponds to the RMSE obtained through 5-fold CV with the training database, and the fifth column is the $RMSE_{TST}$ obtained with the testing database. The last column shows the time in minutes used to create each model.

As one can observe, there is a clear equivalence between the crossed validation error and the error obtained with the testing database, which was not used during the process of training and selecting the best models. None of the $RMSE_{TST}$ surpass the maximum value of the output by more than 0.5%, which indicates that the models generalize correctly.

Model	*Min*	*Max*	*$RMSE_{CV}$*	*$RMSE_{TST}$*	*time (min)*
Cost (€/m²)	9.366287	80.725180	0.100791	0.084571	1560
Energy (MJ/m²)	275.383600	3964.099000	4.650524	4.106709	1403
Emissions ($kgCO_2/m^2$)	17.970540	239.924000	0.258570	0.244703	3250
Rigidity	0.006684	9.204027	0.007447	0.005897	4606
Deflection (cm)	0.005849	14.956540	0.010896	0.009559	1671

Table 5. Results obtained for each model.

3.3 Searching for Optimum Solutions for each Output

The MetaDL, which is obtained as described in the above section, is then utilized to search for optimum outputs for the geometry and loads of each type of slab used in the case study. The process of searching for optimum solutions begins by defining the slab parameters (i-n-c-h) to then obtaining an infinite number of possible solutions by defining the ranges for each of the parameters and varying the values centimeter by centimeter. Thus, in the practical case, the inter-axis varied between 60 and 90 cm, the rib between 10 and 18 cm, the compression layer between 5 and 8 cm, and expanded polystyrene between 15 and 40 cm. The combination of these parameters produced 40,176 possible designs for each floor. Table 6 includes the i-n-c-h design that offered the best mono-criteria solutions according to minimum cost, minimum embodied energy and minimum CO_2 emissions per floor.

		€/m²	i-n-c-h	Energy MJ/m²	i-n-c-h	Emissions kgCO₂/m²	i-n-c-h
R	Y	14.57	61-11-5-15	446.73	82-15-5-15	28.72	84-10-5-18
	Z	20.02	61-13-5-23	630.09	74-14-5-24	37.15	90-10-5-29
SR	Y	17.37	61-16-5-17	550.16	80-16-5-19	33.55	90-10-5-24
	Z	24.28	70-17-5-28	769.54	60-12-5-30	43.81	90-10-5-36
D	Y	16.30	62-18-5-15	515.36	84-18-5-17	31.75	90-10-5-22
	Z	22.78	66-16-5-26	718.92	67-13-5-28	41.64	90-10-5-34
CU	Y	19.32	63-16-5-20	613.81	66-13-5-22	36.56	90-10-5-27
	Z	27.04	90-10-5-31	858.97	74-15-5-34	48.68	90-10-5-40
G	Y	16.25	67-16-5-16	515.78	89-16-5-18	31.70	90-10-5-22
	Z	22.61	66-15-5-26	718.07	71-13-5-28	41.44	90-10-5-33

R: Roof, SR: Storage room, D: Dwellings, CU: Commercial use, G: Garages.

Table 6. Optimum slab design in terms of cost, embodied energy and emissions for buildings Y and Z.

In order to comply with regulations, those solutions wherein the ratio of deflection was greater than 1 were discarded, that is, those cases that presented deflection levels greater than the admissible level. Similarly, using lighteners such as expanded polystyrene requires compression layers of at least 5 centimeters. Thus, the results shown in Table 6 correspond to the minimums obtained after eliminating those cases that did not comply with the above-mentioned restrictions.

The different solutions shown in Table 6 are the individual optimum solutions per floor according to the three parameters analyzed. **Es habitual construir los edificios empleando un único tipo de forjado unidireccional**. Table 7 shows the average values per square meter obtained for both buildings according to **an unique** design and compares them to the values obtained with the methodology utilizing the optimization criteria**. En la primera fila de la tabla se muestran los resultados promedio obtenidos para el diseño 72-12-5-25. En el resto de las filas se identifican en negrita los resultados óptimos según el criterio de diseño: costs, energy or emissions. Para las soluciones obtenidas se aporta el resultado promedio en el resto de indicadores.**

	Building Y			Building Z		
Design Criteria	€/m²	MJ/m²	kgCO₂/m²	€/m²	MJ/m²	kgCO₂/m²
72-12-5-25	19.88	606.88	37.19	24.64	868.75	52.23
Cost	**16.76**	535.65	35.67	**23.34**	758.73	46.94
Energy	16.90	**528.37**	34.18	23.48	**739.12**	45.46
Emissions	17.85	547.67	**32.46**	24.51	759.53	**42.54**

Table 7. Global data for buildings according to optimization strategy.

The results of each optimization strategy, as compared to the use of a single slab design, show that cost optimization for building Y achieved a 15.67% reduction, whereas in building Z costs decreased 5.25%. At the same time, embodied energy decreased 11.74% for building Y and 12.66% for building Z. On the other hand, CO_2 emissions decreased in both buildings: 4.08% in building Y and 10.12% in building Z. Optimizing costs was clearly significant for building Y, though CO_2 emissions did not improve substantially; meanwhile the results for building Z were just the opposite. Both buildings achieved similar improvements for embodied energy.

The results obtained for embodied energy optimization improved 12.94% for building Y and 14.92% for building Z. CO_2 emissions decreased substantially for both buildings (8.10% in Y and 12.96% in Z). Economic savings were greater for building Y, at 14.98%, than for building Z, at 4.68%.

In terms of CO_2 emissions, the optimization strategy improved by 18.55% for building Z and 12.73% for building Y. However, regarding cost, building Z improved by just 0.51%, whereas building Y by 10.20%. And finally, each building obtained similar reductions in embodied energy values: 9.76% in building Y and 12.57% in building Z.

It should be noted that the solutions examined herein represent extreme cases; in practice, designers can impose different conditions on the design, forcing or limiting the slab's parametric values according to their necessities.

3.4 Multi-objective Selection by analyzing Pareto-optimal Solutions

The previous section outlined the examples based on one design criteria. This section describes the methodology for multi-objective selection based on cost, embodied energy and CO_2 emissions.

To facilitate a multi-objective analysis, a search for the Pareto-optimal solutions is realized, which limits the number of solutions to a manageable amount for designers. For example, Table 8 lists the Pareto-optimal solutions for the CU floor of building Y. Also, Figure 7 shows with red points the Pareto front for the same floor. In this case, the optimal Pareto values are derived from those cases of rigidity less than or equal to 1 and considering three objective output variables (Cost €/m^2, Energy MJ/m^2 y Emissions $kgCO_2/m^2$).

i.n.c.h	Use (kN/m^2)	Pavement (kN/m^2)	Partition (kN/m^2)	Span (cm)	Cost €/m^2	Energy MJ/m^2	Emissions $kgCO_2/m^2$	Ratio Deflection	Deflection (cm)
60-15-5-20	4	1	2	420	19.34	621.56	40.69	0.98	1.04
63-16-5-20	4	1	2	420	19.32	620.27	40.85	0.97	1.02
62-14-5-21	4	1	2	420	19.35	616.48	39.75	0.96	0.99
63-14-5-21	4	1	2	420	19.34	617.91	39.60	0.98	1.01
61-12-5-22	4	1	2	420	19.43	615.29	38.82	0.98	1.01
62-12-5-22	4	1	2	420	19.42	618.35	38.85	1.00	1.03
66-13-5-22	4	1	2	420	19.42	613.81	38.82	0.99	1.01
64-11-5-23	4	1	2	420	19.57	619.58	38.31	0.99	1.02
68-12-5-23	4	1	2	420	19.59	615.91	38.30	0.97	1.00
69-12-5-23	4	1	2	420	19.58	616.53	38.25	0.98	1.02
70-12-5-23	4	1	2	420	19.57	619.22	38.32	0.99	1.04
74-13-5-23	4	1	2	420	19.62	615.32	38.29	0.98	1.01
75-13-5-23	4	1	2	420	19.60	615.97	38.23	0.99	1.02
64-10-5-24	4	1	2	420	19.81	620.97	37.77	0.97	1.00
65-10-5-24	4	1	2	420	19.79	621.72	37.76	0.99	1.02
77-12-5-24	4	1	2	420	19.76	620.06	37.78	0.98	1.02

78-12-5-24	4	1	2	420	19.74	621.11	37.78	0.99	1.03
79-12-5-24	4	1	2	420	19.73	622.85	37.83	1.00	1.04
83-13-5-24	4	1	2	420	19.76	619.40	37.86	0.97	1.01
84-13-5-24	4	1	2	420	19.75	619.99	37.79	0.99	1.02
86-12-5-25	4	1	2	420	20.00	622.58	37.30	0.98	1.02
87-12-5-25	4	1	2	420	19.98	622.97	37.26	0.99	1.03
80-10-5-26	4	1	2	420	20.24	627.30	36.87	0.99	1.03
81-10-5-26	4	1	2	420	20.23	628.14	36.84	0.99	1.04
88-11-5-26	4	1	2	420	20.22	626.79	36.91	0.98	1.03
89-11-5-26	4	1	2	420	20.22	627.62	36.91	0.99	1.04
88-10-5-27	4	1	2	420	20.45	630.84	36.64	0.98	1.02
89-10-5-27	4	1	2	420	20.44	630.89	36.57	0.99	1.03
90-10-5-27	4	1	2	420	20.45	631.87	36.56	0.99	1.04

Table 8. Pareto-optimal solutions for the CU floor in building Y.

		Number of initial solutions	Number of Pareto-optimal solutions
R	Y	28892	22
	Z	20691	15
SR	Y	28761	32
	Z	25144	56
D	Y	27861	32
	Z	24652	42
CU	Y	25588	29
	Z	19351	107
G	Y	27786	27
	Z	24559	28

Table 9. Number of valid solutions and Pareto-optimal solutions for each floor of buildings Y and Z.

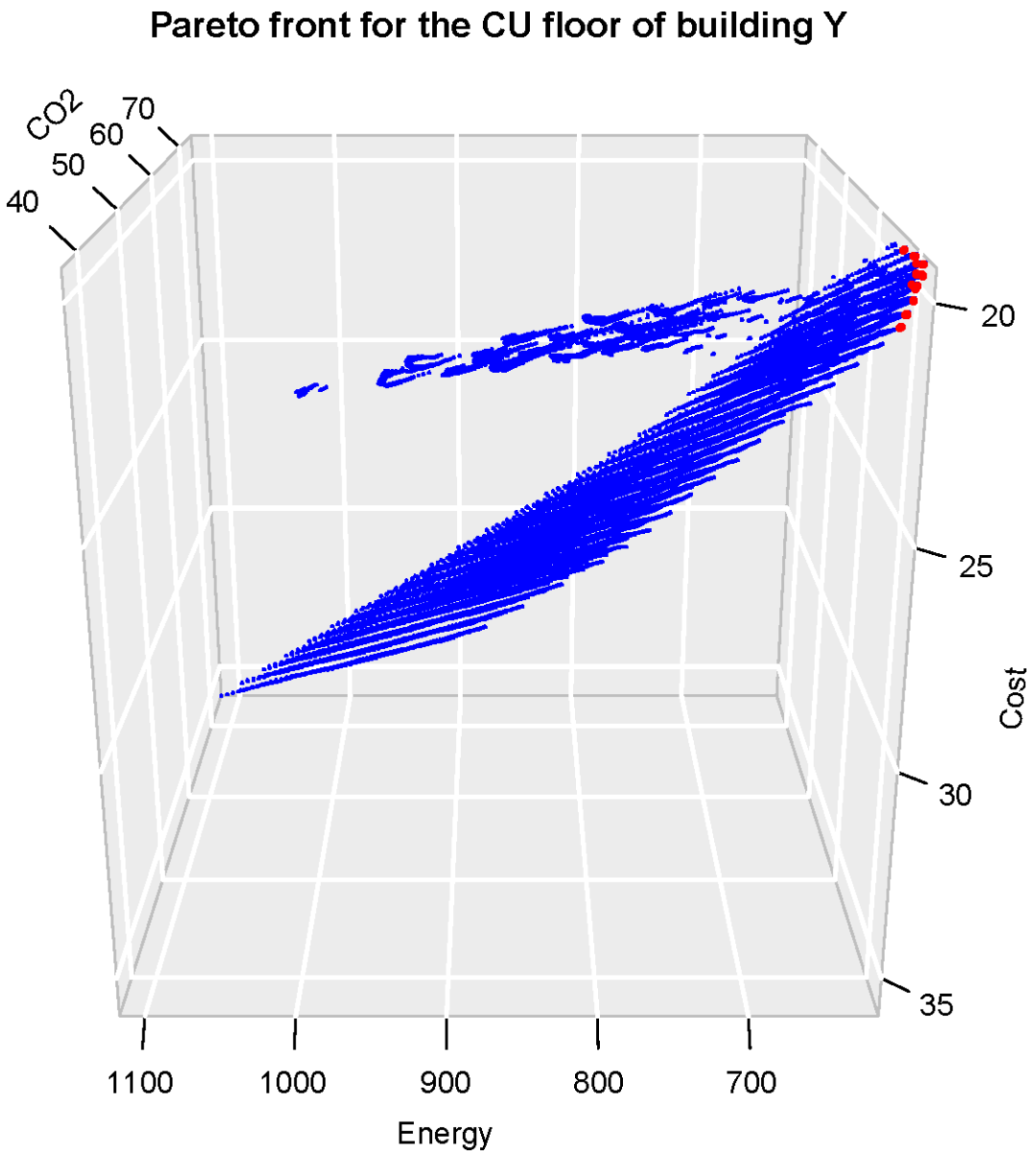

Figure 7. Pareto front (red points) for the CU floor of building Y.

Table 9 shows the number of Pareto-optimal solutions obtained for each floor and building as compared to the number of possible design solutions. As one can observe, the number of solutions decreases enormously; thus the number of final solutions is quite manageable. Based on these solutions, the DSS presents a dendrogram for each floor and building like the one in Figure 7 where the solutions are shown according to their degree of proximity for the CU floor of building Y. This diagram shows the Euclidean distances (height) among the three normalized dimensions (cost, energy and CO_2) of the solutions in a hierarchal format. Logically, neighboring solutions can have similar designs, which is easy to perceive in this type of graph.

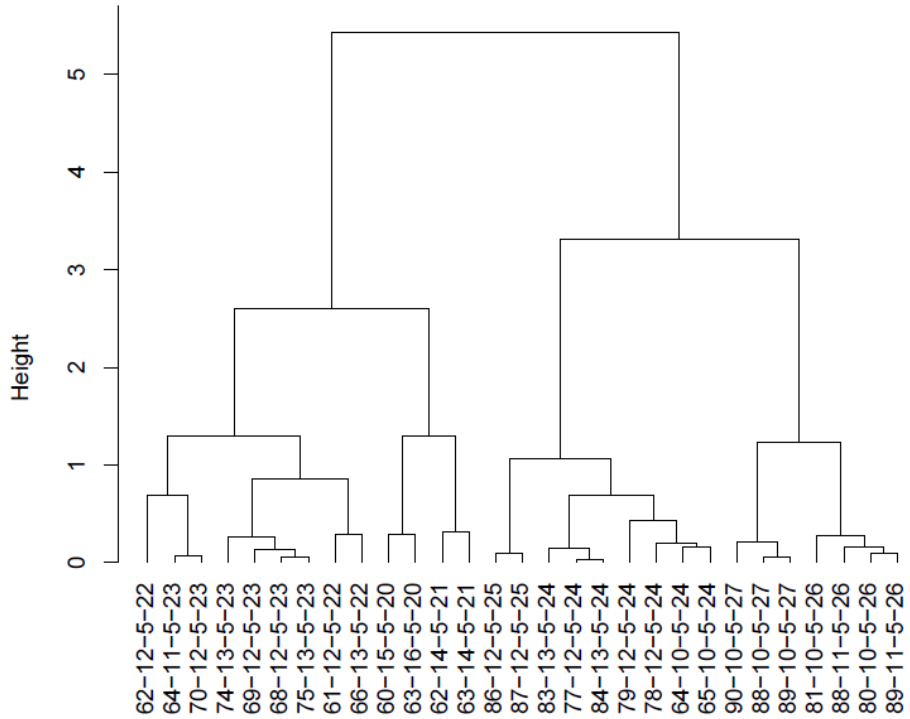

Figure 7. Dendrogram of Pareto-optimal solutions obtained for the CU floor of building Y.

Then, designers can, by referring to the range of solutions (Pareto border) and their criteria, select those solutions that offer the best qualities. For example, continuing with the example of the CU floor design in building Y, the designer can eliminate the solutions with costs greater than +0.15 € over the minimum cost, thereby further reducing the number of final solutions. Figure 8 shows an example of how to use scatter-plots for these cases. The lower triangular region shows scatterplots with pairwise comparisons of the best solutions. A histogram of the values of each variable is displayed diagonally. And finally, in the upper triangular area, the existing correlation between said variables is represented. For example, 0.91 corresponds to the correlation between cost and CO_2 emissions, and the graph in the lower left-hand corner represents the design solutions selected where axis *x* and *y* correspond to cost and CO_2 emissions respectively. Thus, with this tool, designers can select the solution that best adapts to their needs in terms of costs, energy and CO_2 emissions.

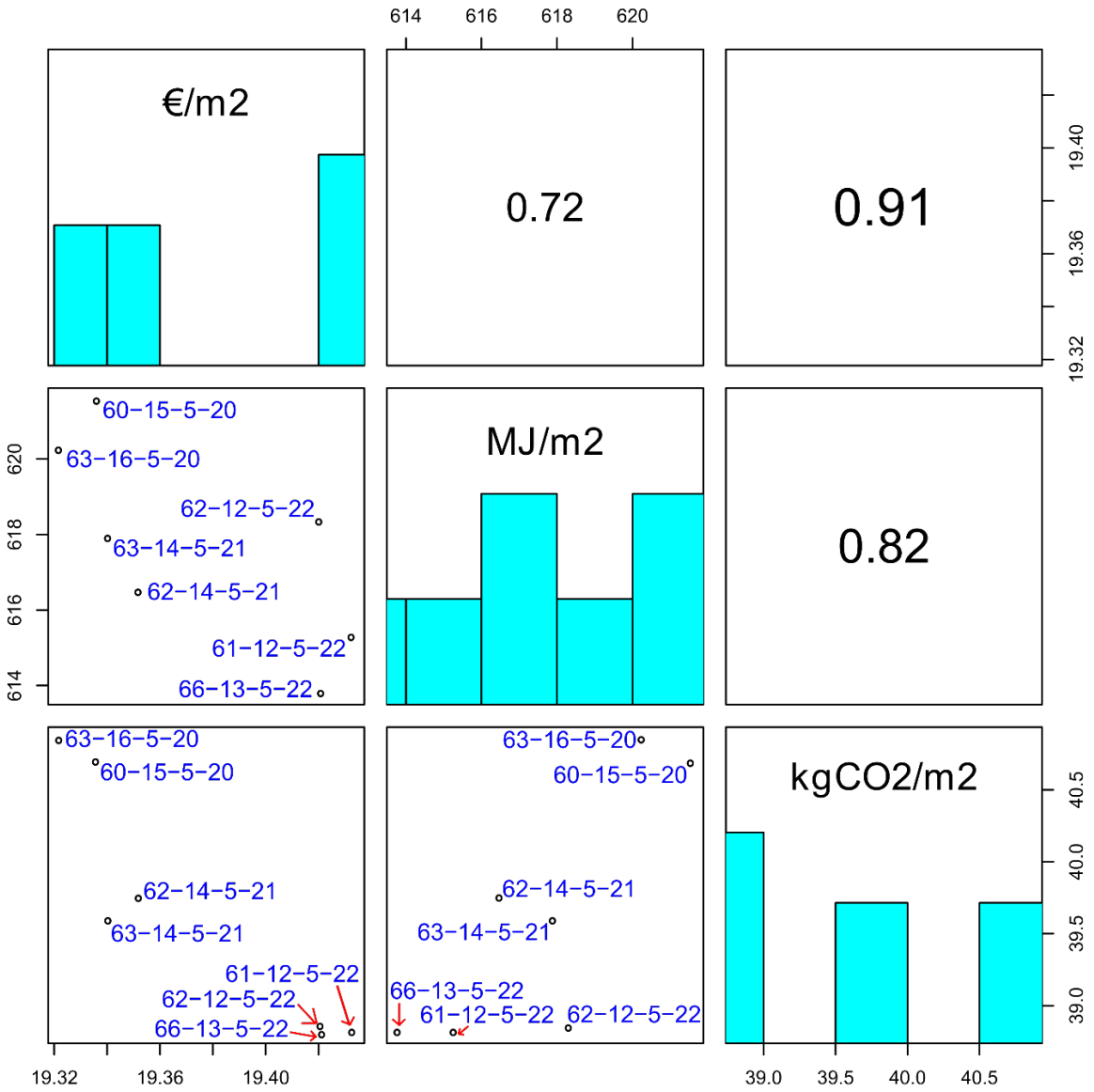

Figure 8. Scatterplot of the most economic solutions for the CU floor of building Y.

According to this methodology, the solution that generates the least impact (embodied energy and CO_2 emissions) is selected for each floor and building. Table 10 shows the results obtained for the slab design of each floor in the buildings.

		Cost €/m²	Energy MJ/m²	Emissions kgCO₂/m²	i-n-c-h
R	Y	14.60	447.10	29.66	76-14-5-15
	Z	20.14	630.90	39.07	75-14-5-24
SR	Y	17.48	551.07	35.45	76-15-5-19
	Z	24.40	769.59	47.09	71-14-5-30
D	Y	16.41	515.75	33.77	85-18-5-17
	Z	22.89	719.52	44.44	72-14-5-28
CU	Y	19.42	613.81	38.82	66-13-5-22
	Z	27.17	859.68	52.23	85-17-5-34
G	Y	16.39	517.68	33.63	88-18-5-17
	Z	22.74	718.07	43.89	71-13-5-28

R: Roof, SR: Storage room, D: Dwellings, CU: Commercial use, G: Garages.

Table 10. Optimal slab design in terms of cost, embodied energy and emissions for buildings Y and Z.

And lastly Table 11 lists the average values for each of the buildings proposed according to the same design (72-12-5-25) and according to the designs developed with the multi-criteria analysis.

	Building Y			Building Z		
Optimization Method	€/m²	MJ/m²	kgCO_2/m²	€/m²	MJ/m²	kgCO_2/m²
72-12-5-25	19.88	606.88	37.19	24.64	868.75	52.23
Cost+Energy+Emissions	16.86	529.08	34.27	23.47	739.55	45.38

Table 11. Global data for buildings according to multi-criteria optimization

Hence, a cost reduction of 15.18% is obtained for building Y and there is 12.82% decrease in embodied energy and 7.86% in CO_2 emissions as compared to the initial design. In the case of building Z, the cost reduction was less (4.75%), though better results are obtained for embodied energy and CO_2 emissions, which decreased 14.87% and 13.11% respectively.

If the multi-criteria solutions are compared to the mono-criteria solutions, the differences are not very significant. Thus, for building Y, the final multi-criteria cost entails a 0.10 €/m² increase over the optimal mono-criteria solution, which had a slight increase in embodied energy (0.13%) compared to the global minimum and a 5.58% increase in CO_2 emissions over the minimum possible emissions. Likewise, the multi-criteria solution for building Z entails just 0.13 €/m² increase in cost, a 0.06% increase in embodied energy, and an increase in CO_2 emissions of 6.68% as compared to the optimal solution. Clearly, the proposed methodology provides solutions that offer significant reductions in embodied energy and CO_2 emissions, at a cost similar to the lowest cost solutions.

4. CONCLUSIONS

This article presents a methodology to develop and apply metamodels based on DL techniques that are capable of condensing the implicit knowledge contained in databases comprised of by millions of construction solutions for one-way slabs. The ultimate objective was to analyze the viability of this type of technique in DSS tools that facilitate the optimization of one-way slabs from a multi-criteria perspective.

This study illustrates this methodology with an example of two buildings of different characteristics. The process began with a heuristic algorithm that calculated over a million construction solutions for one-way slabs representing the universe of existing solutions. Based on this database, a Meta-DL was created consisting of five DNN capable of predicting deflection, rigidity, cost, embodied energy and CO_2 emissions with a high degree of precision for the design of slabs and the loads to which they are subject. In all cases, the DL algorithms were capable of obtaining models with a prediction error of 0.5% using the testing database, thereby demonstrating the strong capacity of these techniques for generalization.

Once the Meta-DL was created, thousands of solutions for the slabs for each floor were created according to the pre-established loads; and those solutions which did not comply with the deflection and rigidity criteria were eliminated. Then, with the remaining solutions, a mono-criteria selection was realized for the optimal slab design for each floor, which in some cases exhibited a significant decrease in cost, embodied energy and CO_2 emissions as compared to the traditional method of using one design for all the slabs in an entire building. For example, in building Y, costs decreased by 15.67%. Similarly, in building Z, although the maximum cost reduction was relatively small, at 5.25%, embodied energy and CO_2 emissions decreased substantially, at 14.92% and 18.55% respectively.

Finally, by using the Pareto-optimal solutions and graphic tools, one can determine the most adequate solutions from a multi-objective standpoint: achieving significant reductions in embodied energy and CO_2 emissions, without incurring significant cost increases as compared to monocriteria solutions.

These results clearly demonstrate the excellent potential for incorporating DL-based metamodels into structural design support tools.

5. REFERENCES

[1] A. Dimoudi and C. Tompa, “Energy and environmental indicators related to construction of office buildings,” *Resour. Conserv. Recycl.*, vol. 53, no. 1–2, pp. 86–95, 2008.

[2] X. Cao, X. Dai, and J. Liu, “Building energy-consumption status worldwide and the state-of-the-art technologies for zero-energy buildings during the past decade,” *Energy Build.*, vol. 128, pp. 198–213, 2016.

[3] H. Park, B. Kwon, Y. Shin, Y. Kim, T. Hong, and S. Choi, “Cost and CO2 Emission Optimization of Steel Reinforced Concrete Columns in High-Rise Buildings,” *Energies*, vol. 6, no. 11, pp. 5609–5624, Oct. 2013.

[4] F. J. Martinez-Martin, F. Gonzalez-Vidosa, A. Hospitaler, and V. Yepes, “Multi-objective optimization design of bridge piers with hybrid heuristic algorithms,” *J. Zhejiang Univ. Sci. A*, vol. 13, no. 6, pp. 420–432, Jun. 2012.

[5] C. V. Camp and A. Assadollahi, “CO2 and cost optimization of reinforced concrete footings subjected to uniaxial uplift,” *J. Build. Eng.*, vol. 3, pp. 171–183, Sep. 2015.

[6] M. Khajehzadeh, M. R. Taha, and M. Eslami, “A New Hybrid Firefly Algorithm for Foundation Optimization,” *Natl. Acad. Sci. Lett.*, vol. 36, no. 3, pp. 279–288, Jun. 2013.

[7] M. Khajehzadeh, M. R. Taha, and M. Eslami, “Efficient gravitational search algorithm for optimum design of retaining walls,” *Struct. Eng. Mech.*, vol. 45, no. 1, pp. 111–127, 2013.

[8] V. Yepes, F. Gonzalez-Vidosa, J. Alcala, and P. Villalba, “CO2-Optimization Design of Reinforced Concrete Retaining Walls Based on a VNS-Threshold Acceptance Strategy,” *J. Comput. Civ. Eng.*, vol. 26, no. 3, pp. 378–386, May 2012.

[9] C. Torres-Machi, V. Yepes, J. Alcalá, and E. Pellicer, “Optimization of high-performance concrete structures by variable neighborhood search,” *Int. J. Civ. Eng.*, vol. 11, no. 2 A, pp. 90–99, 2013.

[10] I. Paya-Zaforteza, V. Yepes, A. Hospitaler, and F. González-Vidosa, “CO2-optimization of reinforced

concrete frames by simulated annealing," *Eng. Struct.*, vol. 31, no. 7, pp. 1501–1508, Jul. 2009.

[11] I. Merta and S. Kravanja, "Cost Optimum Design of Reinforced Concrete Simply Supported One-Way Slabs," in *Earth and Space 2010*, 2010, vol. 93, pp. 2670–2678.

[12] S. M. R. Tabatabai and K. M. Mosalam, "Computational platform for non-linear analysis/ optimal design of reinforced concrete structures," *Eng. Comput.*, vol. 18, no. 5/6, pp. 726–743, Aug. 2001.

[13] A. Kaveh and A. Shakouri Mahmud Abadi, "Cost Optimization of Reinforced Concrete One-Way Ribbed Slabs Using Harmony Search Algorithm," *Arab. J. Sci. Eng.*, vol. 36, no. 7, pp. 1179–1187, 2011.

[14] A. Kaveh and A. F. Behnam, "Cost optimization of a composite floor system, one-way waffle slab, and concrete slab formwork using a charged system search algorithm," *Sci. Iran.*, vol. 19, no. 3, pp. 410–416, Jun. 2012.

[15] A. Kaveh and S. Bijari, "Optimum cost design of reinforced concrete one-way ribbed slabs using CBO, PSO and democratic PSO algorithms," *Asian J. Civ. Eng.*, vol. 15, no. 6, pp. 788–802, 2014.

[16] A. Kaveh and M. H. Ghafari, "Optimum design of steel floor system: Effect of floor division number, deck thickness and castellated beams," *Struct. Eng. Mech.*, vol. 59, no. 5, pp. 933–950, 2016.

[17] B. Ahmadi-Nedushan and H. Varaee, "Minimum cost design of concrete slabs using particle swarm optimization with time varying acceleration coefficients," *World Appl. Sci. J.*, vol. 13, no. 12, pp. 2484–2494, 2011.

[18] O. Liébana, M. D. G. Pulido, and J. Gómez-Hermoso, "CO2 emissions analysis from in situ concrete one-way flat slabs production," *Inf. la Construcción*, vol. 67, no. 539, p. e096, Sep. 2015.

[19] J. J. J. del Coz Díaz, P. J. J. García Nieto, J. Domínguez Hernández, and A. Suárez Sánchez, "Thermal design optimization of lightweight concrete blocks for internal one-way spanning slabs floors by FEM," *Energy Build.*, vol. 41, no. 12, pp. 1276–1287, Dec. 2009.

[20] E. Fraile-Garcia, J. Ferreiro-Cabello, E. Martinez-Camara, and E. Jimenez-Macias, "Optimization based on life cycle analysis for reinforced concrete structures with one-way slabs," *Eng. Struct.*, vol. 109, pp. 126–138, Feb. 2016.

[21] J.-S. Chou, N.-T. Ngo, and A.-D. Pham, "Closure to 'Shear Strength Prediction in Reinforced Concrete Deep Beams Using Nature-Inspired Metaheuristic Support Vector Regression' by Jui-Sheng Chou, Ngoc-Tri Ngo, and Anh-Duc Pham," *J. Comput. Civ. Eng.*, vol. 30, no. 1, p. 7015002, Jan. 2016.

[22] G. Yavuz, "Shear strength estimation of RC deep beams using the ANN and strut-and-tie approaches," *Struct. Eng. Mech.*, vol. 57, no. 4, 2016.

[23] A. Fiore, G. Quaranta, G. C. Marano, and G. Monti, "Evolutionary Polynomial Regression–Based Statistical Determination of the Shear Capacity Equation for Reinforced Concrete Beams without Stirrups," *J. Comput. Civ. Eng.*, vol. 30, no. 1, p. 4014111, Jan. 2016.

[24] I. F. Kara, "Empirical modeling of shear strength of steel fiber reinforced concrete beams by gene expression programming," *Neural Comput. Appl.*, vol. 23, no. 3–4, pp. 823–834, Sep. 2013.

[25] M. Słoński, "A comparison of model selection methods for compressive strength prediction of high-performance concrete using neural networks," *Comput. Struct.*, vol. 88, no. 21–22, pp. 1248–1253, Nov. 2010.

[26] H. Yaprak, A. Karacı, and İ. Demir, "Prediction of the effect of varying cure conditions and w/c ratio on the compressive strength of concrete using artificial neural networks," *Neural Comput. Appl.*, vol. 22, no. 1, pp. 133–141, Jan. 2013.

[27] H. Dilmaç and F. Demir, "Stress–strain modeling of high-strength concrete by the adaptive network-based fuzzy inference system (ANFIS) approach," *Neural Comput. Appl.*, vol. 23, no. S1, pp. 385–390, Dec. 2013.

[28] M. H. Severcan, “Prediction of splitting tensile strength from the compressive strength of concrete using GEP,” *Neural Comput. Appl.*, vol. 21, no. 8, pp. 1937–1945, Nov. 2012.

[29] L. Bal and F. Buyle-Bodin, “Artificial neural network for predicting creep of concrete,” *Neural Comput. Appl.*, vol. 25, no. 6, pp. 1359–1367, Nov. 2014.

[30] O. Gencel, F. Kocabas, and J. J. del Coz Diaz, “A comparative modeling study to estimate wear of concrete,” *Neural Comput. Appl.*, vol. 24, no. 3–4, pp. 649–662, Mar. 2014.

[31] M.-Y. Cheng and N.-D. Hoang, “Risk Score Inference for Bridge Maintenance Project Using Evolutionary Fuzzy Least Squares Support Vector Machine,” *J. Comput. Civ. Eng.*, vol. 28, no. 3, p. 4014003, May 2014.

[32] N. M. Okasha and D. M. Frangopol, “Advanced Modeling for Efficient Computation of Life-Cycle Performance Prediction and Service-Life Estimation of Bridges,” *J. Comput. Civ. Eng.*, vol. 24, no. 6, pp. 548–556, Nov. 2010.

[33] G. C. Marano, G. Quaranta, and M. Mezzina, “Fuzzy Time-Dependent Reliability Analysis of RC Beams Subject to Pitting Corrosion,” *J. Mater. Civ. Eng.*, vol. 20, no. 9, pp. 578–587, Sep. 2008.

[34] L. Sadowski and M. Nikoo, “Corrosion current density prediction in reinforced concrete by imperialist competitive algorithm,” *Neural Comput. Appl.*, vol. 25, no. 7–8, pp. 1627–1638, Dec. 2014.

[35] V. Yepes, T. García-Segura, and J. M. Moreno-Jiménez, “A cognitive approach for the multi-objective optimization of RC structural problems,” *Arch. Civ. Mech. Eng.*, vol. 15, no. 4, pp. 1024–1036, Sep. 2015.

[36] V. C. Castilho and M. C. V. Lima, “Cost optimisation of lattice-reinforced joist slabs using genetic algorithms,” *Struct. Concr.*, vol. 8, no. 3, pp. 111–118, Sep. 2007.

[37] Y. Z. Hailong Zhao, Zhufeng Yue, Yongshou Liu, Zongzhan Gao, “An efficient reliability method combining adaptive importance sampling and Kriging metamodel,” *Appl. Math. Model.*, vol. 5239, no. 1, pp. 1853–1866, Nov. 2015.

[38] S. Gharehbaghi and M. Khatibinia, “Optimal seismic design of reinforced concrete structures under time-history earthquake loads using an intelligent hybrid algorithm,” *Earthq. Eng. Eng. Vib.*, vol. 14, no. 1, pp. 97–109, Mar. 2015.

[39] H. Yin, H. Fang, Q. Wang, and G. Wen, “Design optimization of a MASH TL-3 concrete barrier using RBF-based metamodels and nonlinear finite element simulations,” *Eng. Struct.*, vol. 114, pp. 122–134, May 2016.

[40] C.-S. Kao and I.-C. Yeh, “Using neural networks to integrate structural analysis package and optimization package,” *Neural Comput. Appl.*, vol. 27, no. 3, pp. 571–583, Apr. 2016.

[41] Ministry of Public Works Spain, *Code on Structural Concrete (Spanish abbreviation – EHE-08)*. 2008.

[42] B. P. Weidema, C. Bauer, R. Hischier, C. Mutel, T. Nemecek, J. Reinhard, C. O. Vadenbo, and G. Wernet, “Data quality guideline for the ecoinvent database version 3,” vol. 3, no. 1, p. 169, 2013.

[43] S. Institute of Construction Technology of Catalonia (ITeC), “BEDEC. Structured Data Bank for Construction Elements.” [Online]. Available: www.itec.es/nouBedec.e. [Accessed: 01-Aug-2016].

[44] CYPE Ingenieros S.A., “CYPE Ingenieros S.A. Software for Architecture, Engineering and Construction. Spain, 2016.” 2017.

[45] Association Steel Sustainability, “GlobalEPD 001-002 rev. 1 ECO EPD Ref. nº: 059.” Spain, 2015.

[46] Holcim Romania, “Environmental Product Declaration (EPD) of Ready-Mix Concrete.” 2014.

[47] Environmental Construction Products Organisation (ECO), “Expanded Polystyrene (EPS) Foam Insulation ECO-EPS-00010101-1106.” 2011.